Available online at www.sciencedirect.com

jmr&t Journal of Materials Research and Technology

www.jmrt.com.br

Original Article

Tension Failure Simulation of Notched Composite Laminate Using Floating Node Method Combined with In-Situ Effect Theory

Kun Tian[a], *Song Zhou*[a,*], *Chaozhi Yang*[a], *Jinhua Zhang*[a], *Chaobin Zhou*[b]

[a] *Harbin Institute of Technology, Harbin, Heilongjiang province, 150001, China*

[b] *College of Mechano-Electronic Engineering, Lanzhou University of Technology, Lanzhou, Gansu province, 730050, China*

ARTICLE INFO

Article history:
Received 2 August 2018
Accepted 19 February 2019
Available online 29 May 2019

Keywords:
In-Situ theory
Floating node method
Notched laminates

ABSTRACT

In order to model the progressive failure of laminates under tensile load, the finite element model adopting the floating node method combined with In-Situ effect strength theory is developed in this paper. The floating node method is based on the original finite elements to assign more additional degree of freedoms on the edges or nodes. In this way, it can realize crack propagation explicitly and prevent the singularity caused by the integration of body elements at the damage points. The calculation method of In-Situ strength theory based on the assumption of fracture mechanics is introduced and deduced, which improves the accuracy of the failure strength prediction. Two kinds of notched composite laminates' tensile experiments were carried out. Experiment results show that different ply sequences ([453/903/-453/03]s and [45/0/-45/90]3s) have different failure strength and failure progress. In this paper, the reliability of the model is verified by comparing the experimental results with the simulation results. The comparison results demonstrate that this model can realize the explicit crack propagation and predict the failure strength precisely. In addition, this model can represent some failure modes such as fiber breakage, matrix damage, and delamination, which were observed from experimental phenomenon. The traditional failure criteria compared to the improved criteria's accuracy is significantly improved. It demonstrated that the analysis in considering the In-Situ effect is very necessary.

1. Introduction

Due to its excellent mechanical properties, fiber reinforced composite laminates are widely used in industry especially in aerospace industry. But the failure mechanism and failure modes are complex, such as matrix cracking and fiber breakage or delamination, the strength design and crack propagation prediction of composite laminates have become the most important problems for designers, especially notched laminates. In order to accurately predict the tensile strength and crack propagation of composite laminates, a reasonable finite element model needs to be established.

When Reifsnider [1] was conducting the fatigue test of composite materials, the concept of composite material damage

* *Corresponding author.*
E-mail: zhousong@hit.edu.cn (S. Zhou).

https://doi.org/10.1016/j.jmrt.2019.02.009

was proposed. Over the years, this concept was introduced in many finite element models, such as Smeared Crack Models (SCMs) [2–4]. The model focuses on the realization of material constitutive relationship and the calculation of deformation after the material degradation of stiffness matrix. The SCMs are effective and stable, which can simulate the complicated crack mode. This method is mainly used for the failure strength prediction of the notched composite laminate, whose failure modes are mainly fiber pull-out and fiber breakage. However, when the failure mode of composite laminate is mainly matrix damage or delamination, the process of intersect of two cracks could not be predicted, this leads to a relatively low strength forecast [4]. It can be seen that SCMs have limited ability to predict the trend and shape of the crack. The direction of the crack is also related to the mesh generation [5]. Therefore, a clear pattern of crack display is an essential step in the accurate prediction of crack propagation. The Extended Finite Element Method (XFEM) [6] and the Phantom Node Method (PNM) proposed by Belytschko and his collaborator [7,8], they all use additional degree of freedoms to simulate the cracks intersect. But they all have the same error in geometrical approximation. To resolving this problem, Chen [9,10] puts forward a new method, the Floating Node Method (FNM). This method has many similarities with PNM in calculating structure. Once damage discontinuities appears, the element will be divided into several sub-elements. FNM has many advantages which PNM does not have [11]: It does not have the distortion of the crack in geometry; the integration of sub-elements is simple, and do not need to convert some of them into the natural coordinate after integration, which can easily contain discontinuity and cohesive elements' cracks. It is the presentation of an ideal and complex network of discontinuous bodies. The concept is simpler. The result is equivalent to the repartition of the mesh in the cracking element. More important, FNM: it is different from PNM in algorithm structure; its repartition mesh is more efficient in computing; you can use the approximate FE (Finite element) code to easily implement it (using user-defined elements).

In the traditional strength theory, scholars usually use the unidirectional laminate tension, compression and shear strength values as the inherent properties of materials for strength criterion, and then predict the strength of the multidirectional laminated plates. But according to a series of tests results Parvizi, Dvorak, Flaggs et al [12–14] found that for the sub-layer with the same laying direction and thickness, the matrix strength (including transverse tensile and shear strength) between the multi-directional laminates and the unidirectional laminates is different, which is higher in the multi-directional laminates. Many papers call this phenomenon In-Situ strength effect. Flaggs and Kural's test results [14] show that, the transverse tensile strength of the sub-layer $[90]_s$is 2.48 times of the unidirectional layer, which the sequence of layers is $[0_2/90]_s$ Dvorak and Laws [13] found that the In-Situ strength of the laminates is also related to the thickness of the layer. The thinner the layer is, the higher the In-Situ strength is. Many scholars gradually realized the importance of In-Situ effect of composite laminates and began to consider this factor in strength theory. Sun and Tao [15] proposed to directly use 1.5 times of the transverse tensile and shear strength values of the unidirectional laminates as the corresponding In-Situ strength, and set up the In-Situ strength criteria to predict the failure of composite laminates. Rotem [16] use 1.2 times of the unidirectional laminates' strength value as the corresponding In-Situ strength. Chang et al. [17] proposed a method to calculate local strength, but this method requires a lot of experiments to fit the material constants required in the formula. Dvorak and Laws [13] proposed a mechanical model and method for calculating In-Situ strength based on fracture mechanics theory. Then Camnbo et al. [18] considered the influence of shear nonlinearity on In-Situ strength calculation, based on Dvorak and Laws. The theoretical model of In-Situ strength proposed by Dvorak and Laws [13] is more scientific and effective than other methods, and it does not require experimental fitting parameters. It is a popular calculation method at present.

In order to simulate the explicit crack propagation process and predict the failure strength precisely, a model using floating node method combined with In-Situ effect theory is set up. As a comparison, a static tensile experiment about two kinds of notched composite laminates is carried out.

2. Failure Theory

2.1. *Floating node method*

Because of the complexity of the composite material, the traditional finite element method such as SCMs [2–4] has some drawbacks. For example, it can't simulate the explicit crack, which uses the damage variables to represent it. Another drawback is that cracks usually propagate along the preset grid path. And another fatal flaw is that, at the fiber fracture point, integration may contain singularity, which leads low computational efficiency. In order to improve these defects, the explicit cracks can be simulated by using some special method —— inserting additional degree of freedoms.

Floating node method [9,10] is based on the traditional finite element method, additional degree of freedoms is inserted at borders and nodes. And the biggest difference between XFEM and FNM is that these additional degrees of freedom can be "floating" on the border. This method obviously realizes the explicit propagation of cracks, which can be represented as the generation of additional Dofs when the cracks through the element.

The specific implementation is as follows:

This paper takes the composite laminates model as an example to introduce this method, Figure 1. A composite

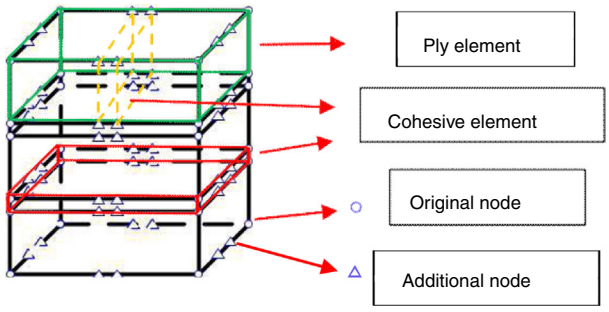

Figure 1 – Additional nodes on the edge.

laminates model can be considered as a large composite material element. And this element can be divided into a fiber layer and a cohesive layer. We use a cohesive layer to simulate inter-layer failures and a fiber layer to simulate normal inner-layer failures. Both the fiber layer and the cohesive layer using floating node method.

A hexahedron element, whose each edge was embedded two additional nodes, but in the initial condition, the element is considered to be "INTAC". At the initiation of the failure, some of the additional nodes are activated by the constitutive laws. Then this hexahedron element will be divided into three parts, consists of two basic finite element elements and a cohesive element. The cohesive element is used to simulate the crack.

Since nodes and boundary information are shared in real time, the damage condition of whole model can be dealt with in each element. According to the constitutive law, the crack initiation can be determined at any time when the stress conditions is satisfied. The propagation of cracks can be determined according to the activation degree of additional nodes within the element's boundary. That is, whether there is new element generation.

2.1.1. *Ply element*

A Ply element can realize some main inner layer failure modes, such as matrix cracking, fiber breaking or fiber pulling out from the matrix. As a result of all of the element's information is from the node interpolation, once the constitutive laws are satisfied, the fiber or matrix damage was initiated. Due to the volume of an element is very small, the crack was produced from the element's geometric center. The activated additional nodes connect the geometric center throughout the element, and two new basic finite element and a cohesive element used to characterize the damage are generated.

2.1.2. *Cohesive element*

A cohesive element is mainly used to simulate inter-layer failure, such as delamination. It is not a bearing part, but its main function is playing the roles of crack propagation. When the top and bottom fiber layer both have cracks appear on the boundary, the cohesive element between them will generate automatically a crack to connect the fracture points. One advantage of this method is that all boundary information shared so that crack propagation explicit can come true.

In order to simplify the calculation, first of all, the same element, crack only through once, when the fracture point (floating node) is near the original node (< 10%), it is incorporated into the original node, equivalent to the original node adding some additional degrees of freedom, which is similar to XFEM.

2.2. *Constitutive law*

According to the above element division theory, the failure modes are mainly classified into inter-layer failures and inner-layer failures. The constitutive laws can be described as damage initiation determination and damage evolution parts. The damage initiation of composite laminates is based on the stress conditions to determine. Fiber breakage is using the maximum stress criteria, matrix cracking is using the Pinho [3] criterion, and the delamination is mainly realized by cohesive element, using ABAQUS's built-in laws.

The specific determination formula is as follows:

2.2.1. Failure criterion

2.2.1.1. *Fiber*

In the theory of tension/compression, the maximum stress criterion is adopted when the fiber failure is mainly used.

$$\begin{cases} \dfrac{\sigma_{11}}{X_T} = 1, \sigma_{11} \geq 0 \\ \dfrac{\sigma_{11}}{X_C} = 1, \sigma_{11} \leq 0 \end{cases} \tag{1}$$

Where XT and XC are the ply tensile strength and the compressive strength in the fiber direction, respectively, s_{11} is the fiber direction stress

2.2.1.2. Matrix

In the matrix part, it is mainly the effect of the positive stress an at the fracture surface on the failure response. So using Pinho criterion [3] to transform the stress condition to the main fracture angles' stress condition, which introduce the stress of t_L, t_T and s_n

$$\left(\frac{\sigma_n}{Y_T}\right)^2 + \left(\frac{\tau_T}{S_T}\right)^2 + \left(\frac{\tau_L}{S_L}\right)^2 = 1, \leftarrow \sigma_n \geq 0 \tag{2}$$

Where Y_T is the tensile strength in the transverse direction, and S_T and S_L are the in-pane shear strength.

2.2.1.3. Delamination

In various numerical models proposed by scholars, the method of cohesive element's fracture mechanics is frequently used most widely. The stiffness of the element is weakened by using the bilinear method. The theory is clearly embedded in ABAQUS and can be used directly. Its core theory is as follows:

According to the ABAQUS user manual, the delamination initiates when it satisfied a quadratic failure discriminant as followed.

$$\left(\frac{T_n}{N}\right)^2 + \left(\frac{T_s}{S}\right)^2 + \left(\frac{T_t}{S}\right)^2 = 1 \tag{3}$$

The principal stress and shear stress are respectively T_n, T_s and T_t. Once the discriminant has been satisfied, the energy method can be used to weaken the stiffness, which is similar to the previous part.

2.2.2. *Stiffness Degradation*

After the determination of the damage initiation, the damage represent of the element becomes the core problem of the floating node method. The general idea to reflect effect on the

model is that the stiffness starts to decrease. The main idea to weaken the stiffness is the combination of SCMs in continuum mechanics model and cohesive element in fracture mechanics. According to the test results, the main damage modes of the sample are divided into two types: inner-layer and inter-layer damage.

That is,

(1) Internal damage: matrix, fiber (tensile/compression)
(2) Delamination

No matter what kind of failure is, the rules of energy law are all satisfied. Therefore, the double-line energy method [19,20] can be used.

All failure modes satisfy the energy formula as below

$$\int_0^{\infty} \sigma_i d\left(D_i\right) = G_i \tag{4}$$

$$D_i = \varepsilon_i l_c \tag{5}$$

i is for three failure modes (fiber, matrix, the delamination failure), a represents

the stress, ε is on behalf of the strain, and D is on behalf of the equivalent strain, l_c represents the characteristic length, G represents the fracture energy. They all can be applied to fiber failure, matrix failure and delamination failure respectively. The application of this expression is at the stiffness failure evolution stage, but the stress peak must be determined at first, that is, at the beginning of the stiffness decay.

In the process of damage propagation, the element's damage energy is equal to the total energy that crack crosses the element.

The attenuation parameters are calculated by using Fig. 2.

However, these constitutive relations do not take into account the effect of In-Situ effect, and the calculated results will be relatively low.

2.3. *In-Situ strength theory*

The unidirectional layer thickness in the composite laminates is assumed to be t, and the width of core microcrack is assumed to be 2d, figure 3.

With the increase of external load, the width of the core microcrack increases. When the width reaches the critical

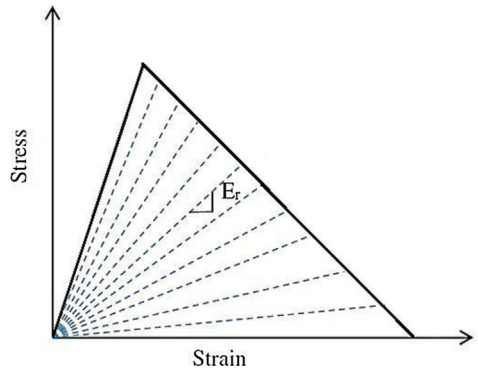

Figure 2 – Bilinear model, stiffness degradation process.

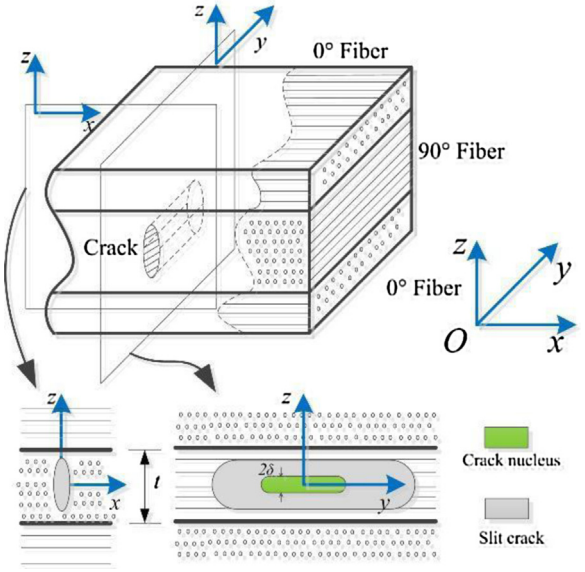

Figure 3 – Fracture mechanics based model.

value of $2d_c$, the microcrack develops into a macroscopic incision crack.

The formation of core microcracks may be caused by the existence of gaps in the matrix, or the debonding between the fiber and the matrix caused by residual stress and manufacturing defects.

When the ply is subjected to transverse stretching or in-plane shear, the propagation direction of core microcrack in 1-3 plane may be along 1 or 3 direction, or in both two directions.

In this paper, the crack extending along 1 direction is called L crack, and the crack along 3 direction is called T crack.

In addition, under the assumption of plane stress, transverse tensile stress s_{22} leads the I-type fracture mode, while the in-plane shear stress s_{12} leads the shear fracture mode.

For orthotropic material, when it is not to consider the influence of the direction of the adjacent layer, Camanho etc. [18] derived an expression for interaction energy W considering shear nonlinear based on the theory proposed by Dvorak and Laws.

The interaction energy W is:

$$W = \frac{1}{2}\pi d^2 \left[\Lambda \sigma_{22}^2 + 2\int_0^{\gamma_{12}} \sigma_{12} d\gamma_{12} \right] = W_I + W_{shear} \tag{6}$$

$$\Lambda = 2\left(\frac{1}{E_{22}} - \frac{\nu_{21}^2}{E_{11}}\right) \tag{7}$$

$$G\left(T\right) = \frac{1}{2}\cdot\frac{\partial W}{\partial d} \tag{8}$$

$$G_I\left(T\right) = \frac{\pi d}{2}\Lambda\sigma_{22}^2 \tag{9}$$

$$G_{shear}\left(T\right) = \pi d\int_0^{\gamma_{12}} \sigma_{12} d\gamma_{12} \tag{10}$$

$$G(L) = \frac{W}{2d} \tag{11}$$

$$G_I(L) = \frac{\pi d}{4}\Lambda\sigma_{22}^2 \tag{12}$$

$$G_{shear}(L) = \frac{\pi d}{2}\int_0^{\gamma_{12}} \sigma_{12} d\gamma_{12} \tag{13}$$

From the derivation above, it is not hard to see that the energy required to drive T crack and L crack is related to the width 2d of core crack in 3 direction, and is independent of the length in 1 direction.

Due to the difference in the thickness and location of the inner unidirectional layer of the composite laminates, the In-Situ strength value will be different. Therefore, unidirectional layer should be divided into three types: embedded thick layer, embedded thin layer and outer surface layer.

Different types of cracks have different directions of propagation, different release rates of crack fracture have different equivalent strength.

2.3.1. Embedded thick ply

If d_{IC} (L) and d_{IC} (T) are respectively to present the type I's L and T direction corresponding the critical crack width value, Dvorak and Laws' study found the relationship that d_{IC} (L) < d_{IC} (T), so in the embedded thick ply, T crack appears earlier than L crack. The core microcracks' width reaches d_{IC} (T), the macroscopic notch crack propagates in the direction of the 3 at first; When the width of the core microcrack reaches d_{IC}(L), the incision crack will propagate simultaneously in the direction of 1 and 3.

From equation (19), the solution is:

$$G_{IC}(T) = \frac{\pi d}{2}\Lambda\left(Y_{is}^T\right)^2 \tag{14}$$

When s22 = Y_{is}T

and $s_{12} = S_{is}{}^L$, the ?$_{12}$ must be given,

However, the nonlinear relationship of in-plane shear is expressed as polynomial

The formula * becomes

$$\gamma_{12} = \frac{\sigma_{12}}{G_{12}} + \beta\sigma_{12}^3 \tag{15}$$

$$G_{shear}(T) = \pi d\int_0^{\gamma_{12}} \sigma_{12} d\gamma_{12} = \pi d\int_0^{S_{is}^L} \sigma_{12}\left(\frac{1}{G_{12}} + 3\beta\sigma_{12}^2\right) d\sigma_{12}$$
$$= \pi d\left[\frac{\left(S_{is}^L\right)^2}{2G_{12}} + \frac{3}{4}\beta\left(S_{is}^L\right)^4\right] \tag{16}$$

The fracture toughness of unidirectional layer is expressed as

$$G_{IC}^*(T) = \left(1.12^2 \times 2\right)\frac{\pi d}{2}\Lambda\left(Y^T\right)^2 \tag{17}$$

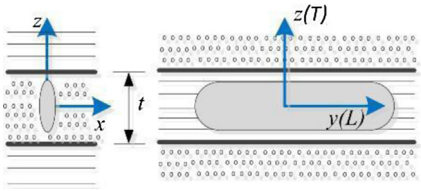

Figure 4 – Schematic diagram of embedded thin ply.

$$G_{shear}^*(T) = 2\pi d\left[\frac{\left(S^L\right)^2}{2G_{12}} + \frac{3}{4}\beta\left(S^L\right)^4\right] \tag{18}$$

By comparing the two equations, it can be solved as:

$$Y_{is}^T = 1.12\sqrt{2}Y^T \tag{19}$$

$$S_{is}^L = \sqrt{\frac{\left(1+\beta\lambda G_{12}^2\right)^{0.5} - 1}{3\beta\lambda G_{12}^2}} \tag{20}$$

$$\lambda = \frac{12\left(S^L\right)^2}{G_{12}} + 18\beta\left(S^L\right)^4 \tag{21}$$

2.3.2. *Embedded thin ply*

The core microcrack in the embedded thin layer in figure 4, due to the unidirectional layer thickness is very thin, was propagating throughout the thickness of thin layer (t ≤ 2 d_{IC}), before it reaches the critical value, but with the increase of load, it still can form the macroscopic notch crack along 1 direction, so the transverse strength of In-Situ can be:

$$G_{IC}(L) = \frac{\pi d}{4}\Lambda\sigma_{22}^2 = \frac{\pi t}{8}\Lambda\left(Y_{is}^T\right)^2 \tag{22}$$

$$Y_{is}^T = \sqrt{\frac{8G_{IC}(L)}{\pi t\Lambda}} \tag{23}$$

$$G_{shear}(L) = \frac{\pi d}{2}\int_0^{\gamma_{12}} \sigma_{12} d\gamma_{12} = \frac{\pi d}{2}\left[\frac{\left(S_{is}^L\right)^2}{2G_{12}} + \frac{3}{4}\beta\left(S_{is}^L\right)^4\right]$$
$$= \pi t\left[\frac{\left(S_{is}^L\right)^2}{8G_{12}} + \frac{3}{16}\beta\left(S_{is}^L\right)^4\right] \tag{24}$$

$$S_{is}^L = \sqrt{\frac{\left(1+\beta\lambda G_{12}^2\right)^{0.5} - 1}{3\beta\lambda G_{12}^2}} \tag{25}$$

$$\lambda = \frac{48G_{shear}(L)}{\pi t} \tag{26}$$

2.3.3. *Outer surface ply*

When the outer surface layer is relatively thin, figure 5, it is considered as a special unconstrained thin layer, also in the classical form of stress strength factor:

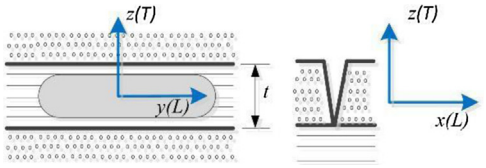

Figure 5 – Schematic diagram of outer surface ply.

Unconstrained thin layer

$$G^*_{IC}(T) = \left(1.12^2 \times 2\right)\frac{\pi t}{8}\Lambda\left(Y^T\right)^2 \tag{27}$$

$$G^*_{shear}(T) = 2\pi t\left[\frac{\left(S^L\right)^2}{8G_{12}} + \frac{3}{16}\beta\left(S^L\right)^4\right] \tag{28}$$

$$Y^T_{is} = 1.79\sqrt{\frac{G_{IC}(L)}{\pi t\Lambda}} \tag{29}$$

$$S^L_{is} = \sqrt{\frac{\left(1+\beta\lambda G^2_{12}\right)^{0.5}-1}{3\beta\lambda G^2_{12}}} \tag{30}$$

$$\lambda = \frac{24G_{shear}(L)}{\pi t} \tag{31}$$

When the outer surface layer s thick, using original strength

$$Y^T_{is} = Y^T \tag{32}$$

$$S^L_{is} = S^L \tag{33}$$

Where, when the thickness of unidirectional layer is much larger than the critical width of core microcrack (i.e., t=2_{dc}), it is defined as thick layer. t<2_{dc} is defined as a thin layer.

According to the analysis results of Dvorak and Laws on carbon-epoxy composite materials, the thickness of unidirectional layer 0.8 mm (or including 5~6 single layers) can be used to distinguish thick layer and thin layer.

According the theory above, it can be summarized as a Table 1 below:

Table 2 – The size of notched laminates.

Length L	Width w	reinforced sheet Length L_0	Hole diameter ?
300mm	38mm	40mm	6.3mm

So the constitutive law of the matrix, the initial damage determination becomes,

$$\left(\frac{\sigma_n}{Y^T_{is}}\right)^2 + \left(\frac{\tau_T}{S_T}\right)^2 + \left(\frac{\tau_L}{S^L_{is}}\right)^2 = 1, \leftarrow \sigma_n \geq 0 \tag{34}$$

In addition, there is no experimental evidence to show that S_T has In-Situ effect in the existing literature, so it is not considered in the above equation.

3. Experiments

3.1. Test specimen

In this paper, the tensile tests of two kinds of notched laminates were carried out. In addition, finite element simulation is carried out using floating node method combined with In-Situ effect theory. In this section, test results and simulation results are presented in detail.

Using notched tensile test method [21,22], two kinds of ply orientation angles laminates are tested. The shape and size are provided in Fig. 6 and Table 2. The tensile test Uses Zwick 10-tonnage unidirectional tensile/compressor to conduct the corresponding damage test. In the tensile test, 10 samples were loaded at a rate of 1.5 mm/min.Fig. 7

Fig. 8 shows the strength of all the specimens. It is found that the damage strength of specimens 1, 2 is very different. The test process, results and stress strain curves of each sample are analyzed and the reasonable explanation is given below.

3.2. The test results of notched laminates [45_3/90_3/-45_3/0_3]s

The ply sequence of laminate is [45_3/90_3/-45_3/0_3]s. The surface is 45° of fiber layer, and the middle is the transition of

Table 1 – Summary of computational methods for transverse tensile and shear In-Situ strength.

Type of ply	Transverse tensile In-Situ strength	Shear In-Situ strength
Embedded thick ply	$Y^T_{is} = 1.12\sqrt{2}Y^T$	$S^L_{is} = \sqrt{\frac{\left(1+\beta\lambda G^2_{12}\right)^{0.5}-1}{3\beta\lambda G^2_{12}}}\lambda = \frac{12\left(S^L\right)^2}{G_{12}} + 18\beta\left(S^L\right)^4$
Embedded thin ply	$Y^T_{is} = \sqrt{\frac{8G_{IC}(L)}{\pi t\Lambda}}$	$S^L_{is} = \sqrt{\frac{\left(1+\beta\lambda G^2_{12}\right)^{0.5}-1}{3\beta\lambda G^2_{12}}}\lambda = \frac{48G_{shear}(L)}{\pi t}$
Outer surface thin ply	$Y^T_{is} = 1.79\sqrt{\frac{G_{IC}(L)}{\pi t\Lambda}}$	$S^L_{is} = \sqrt{\frac{\left(1+\beta\lambda G^2_{12}\right)^{0.5}-1}{3\beta\lambda G^2_{12}}}$ $\lambda = \frac{24G_{shear}(L)}{\pi t}$
Outer surface thick ply	$Y^T_{is} = Y^T$	$S^L_{is} = S^L$
$\beta = 3.6\times10^{-8}MPa^{-3}$		

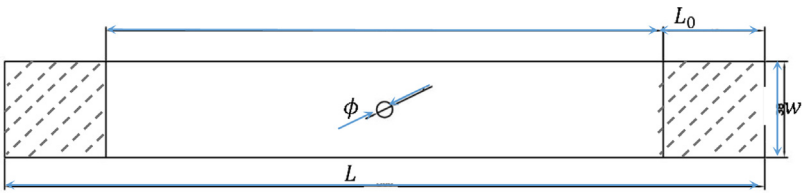

Figure 6 – The shape of notched laminates Table.2. The size of notched laminates.

Figure 7 – Static Materials Testing Machines for the tensile experiments.

the 0 degree fiber layers. In the loading process, the first damage initiated place is the surface around the hole, and a small crack along the 45° direction was first formed on the surface of the hole. Then, as the displacement load increases, the surface warps in the horizontal direction of the hole and begins to appear obvious delamination. At the same time, the crack continues to propagate around the hole's surface. The delamination is more obvious and continues to propagate to the end of the specimen. Cracks appeared on the end surface along the direction of 45 degrees. Finally, the fiber is stripped from the matrix, and the delamination failure mode reaches the end of specimen. The fiber of 0° ply orientation around the hole fractured, which represents the specimen was completely failure.

During the tensile failure test, the sound of crackle of interfacial layer and fiber fracture can be clearly heard.Figure 9, Figure 10

The five specimens have similar gradual damage failure process, and their delamination results are apparent. By using CT scan, it can be clearly seen that they have obvious delamination failure mode in the ply of 90 degrees orientation.

3.3. The test results of notched laminates $[45/0/-45/90]_{3s}$

The surface's ply orientation is a 45-degree, and the whole layer sequence $[45/0/-45/90]_{3s}$ is alternately in the order of [45/0/-45/90]. Compared with the previous specimens, the only difference between them is that there is only one layer in each direction.Figure 11

The final failure form of these 5 samples is the same, all of them have transverse fiber fracture in the center of the hole. During loading process, the failure mode of these 5 specimens is completely different from the previous sequences $[45_3/90_3/-45_3/0_3]_s$, and there is no obvious surface damage. When the loading is almost completely damaged, small crack damage begins to appear on the surface around the hole and at the end of the specimen. At the final failure moment, the fiber near transverse axis of the center of the hole broke. It can be seen from the CT scan, the fracture surface is very neat and nearly brittle.

The damage of the matrix can be seen through the C-scan in only a few layers. It is difficult to see the

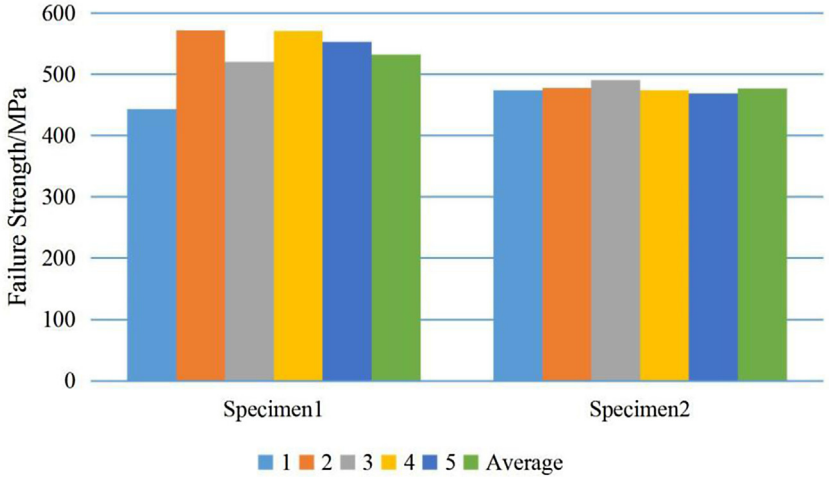

Figure 8 – The experiments results of failure strength.

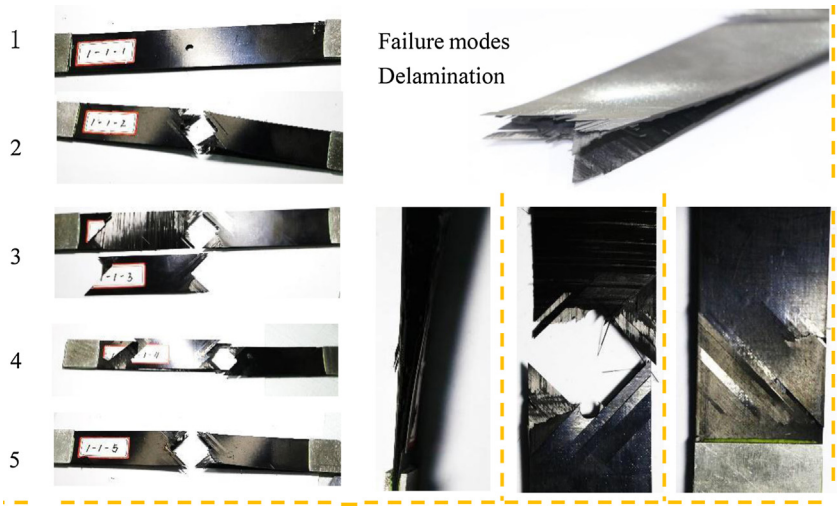

Figure 9 – Delamination and matrix cracking of specimens [453/903/-453/03]s.

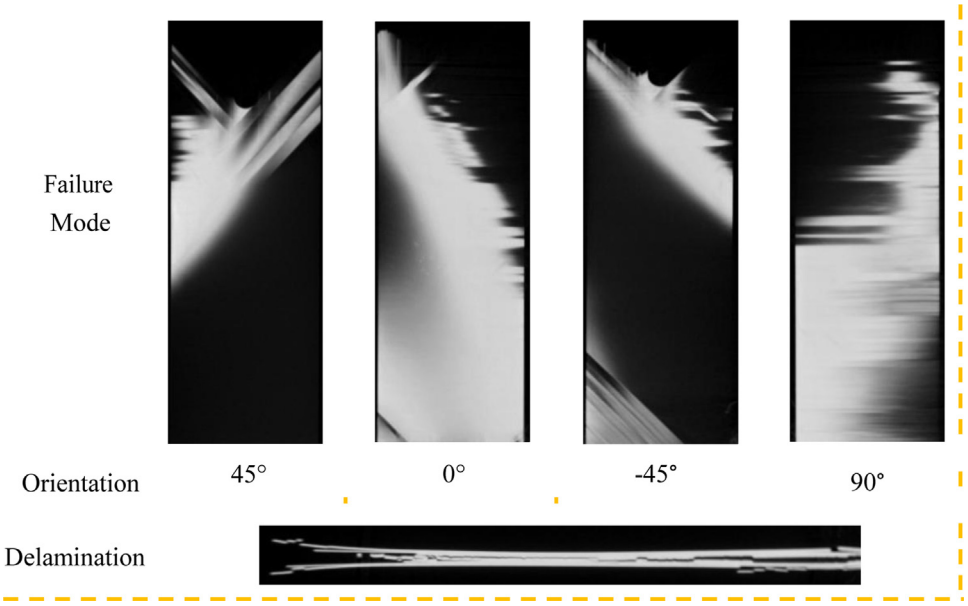

Figure 10 – CT-Scan for each ply of specimen [453/903/-453/03]s.

sequence of the inner layers, and the delamination is not obvious.

The main reason for the difference between the failure modes of layer 1 is that the layering sequence is the alternate. The anisotropy degree is low and the uniformity is higher than first kind of specimen $[45_3/90_3/-45_3/0_3]_s$, so that the delamination is not obvious, and there is main failure mode of fiber fracture.

4. Numerical results

4.1. *Finite element model*

From Fig. 12, the program flow of the model mainly consists of three parts, the first part is the failure initiation's determination, which contains the In-Situ theory, the second part is the element division, and the last part is the stiffness degradation process.

The first part, the failure initiation is determined by ABAQUS solver. ABAQUS solver get solution by using the existing total stiffness matrix, which contains all elements' state of stress and strain. For the fiber elements and cohesive elements, they have a corresponding criteria respectively, see detailed theoretical section 2.2.1. After failure initiation's determination, the failure mode is determined according to the result, which is the matrix cracking, the fiber fracture, or the delamination failure.

The crack propagation is determined according to different failure modes and the location of the crack initiation point. That's the second part, which contains element division and crack propagation, which was discussed in section 2.1.

The last part is the stiffness degradation process. Every user defined element, using the bilinear stiffness

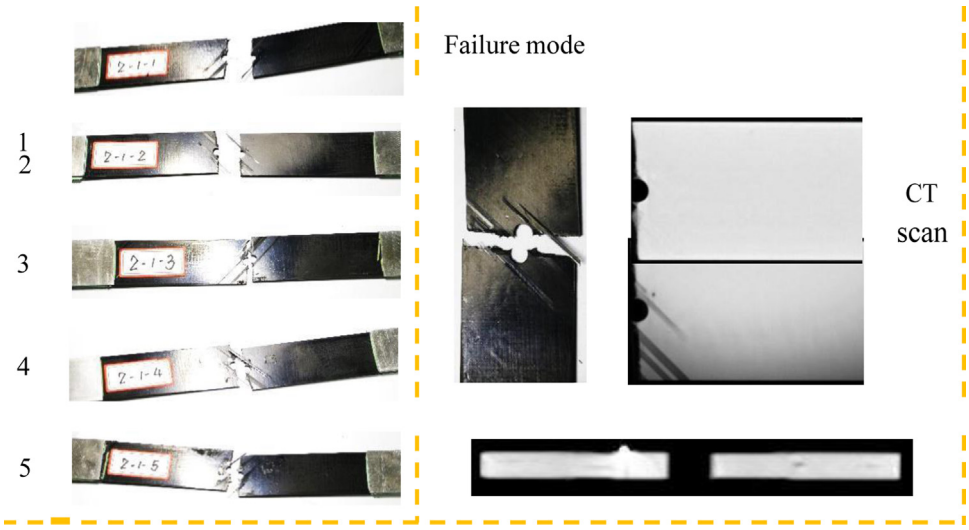

Figure 11 – Test results and CT scan of notched laminates [45/0/-45/90]3s.

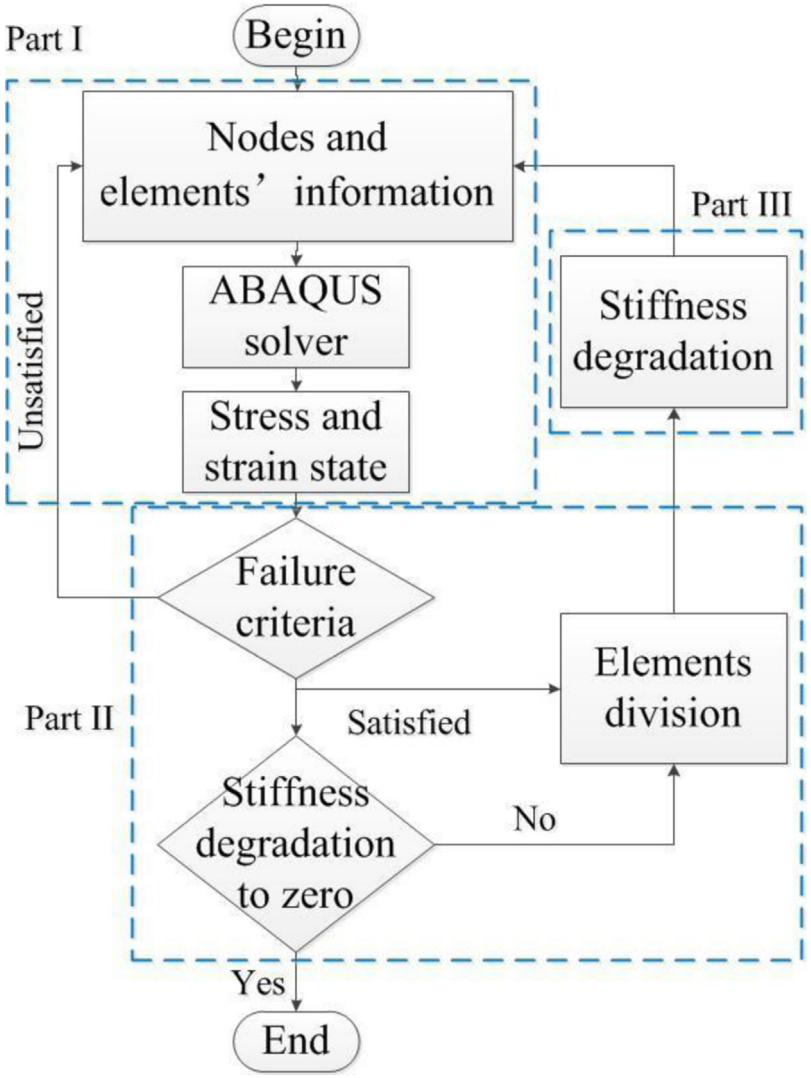

Figure 12 – Main program flow diagram.

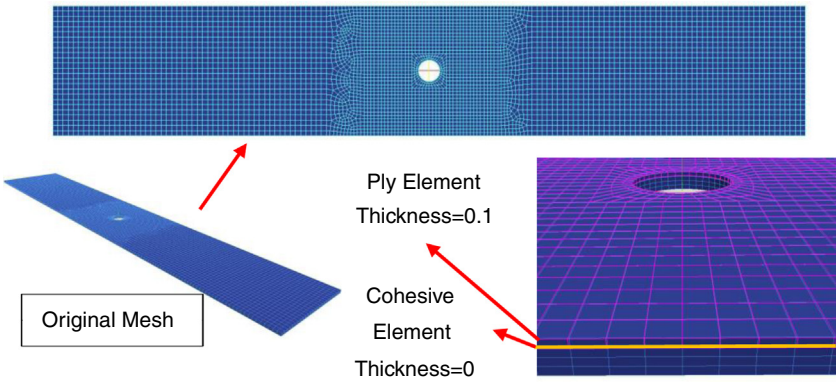

Figure 13 – Mesh of notched laminates.

Table 3 – Input material properties.

parameters	E1/MPa	E2/MPa	G12/MPa	G23/MPa	μ12	μ23
Value	161000	11400	5170	3980	0.34	0.43
parameters	XT/MPa	XC/MPa	YT/MPa	YC/MPa	SL/MPa	ST/MPa
Value	2806	1400	60	185	90	90
parameters	GFCT	GFCC	GNC	GTC	GLC	
Value/N·mm^{-1}	112.7	112.7	0.293	0.631	0.631	

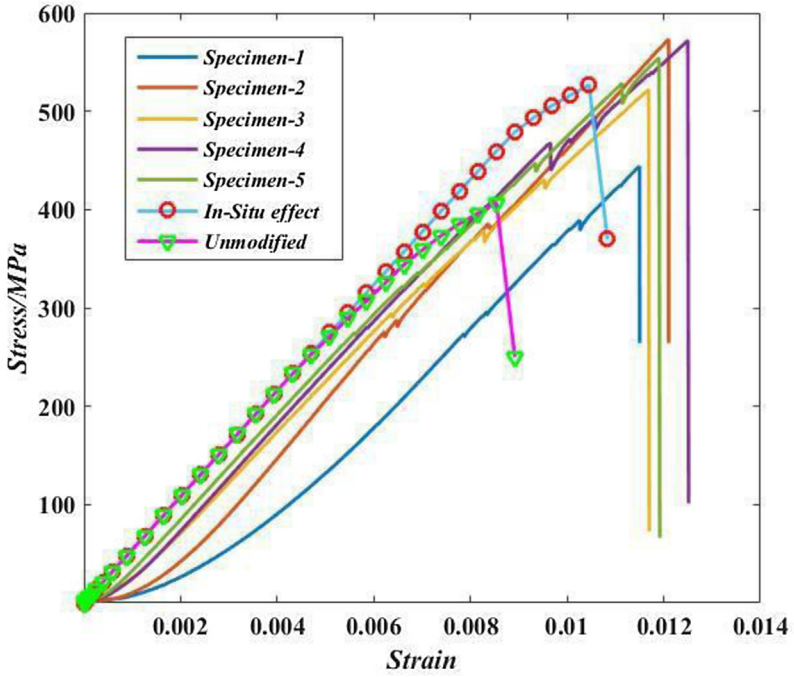

Figure 14 – Simulations and tests' strain-stress curves of specimens $[45_3/90_3/-45_3/0_3]_s$.

degradation rule to calculate stiffness and get assembled, will put the new degraded total stiffness matrix into ABAQUS solver, then get the new state of stress and strain as results.

Repeat the whole program flow from the first part, until the entire model finally fails.

Due to the existence of preprocessing programs written in Python, the modeling process is simpler, and the single-layer model is needed only.Figure 13 Table 3

(1) Here are some things to notice:
(2) The size of the notched tension model is 220 mm x 38 mm, the diameter of the hole is 6.3 mm and the thickness of the single layer is 0.1 mm.
(3) Because each of the composites is 24 layers and the calculation is large, the $[\theta_3]$ layers are used as a simplified layer $[\theta]$. For example, $[45_3/90_3/-45_3/0_3]_s$, which is equivalent to [45/90/-45/0]. In addition, both are symmetric models, which are simplified.

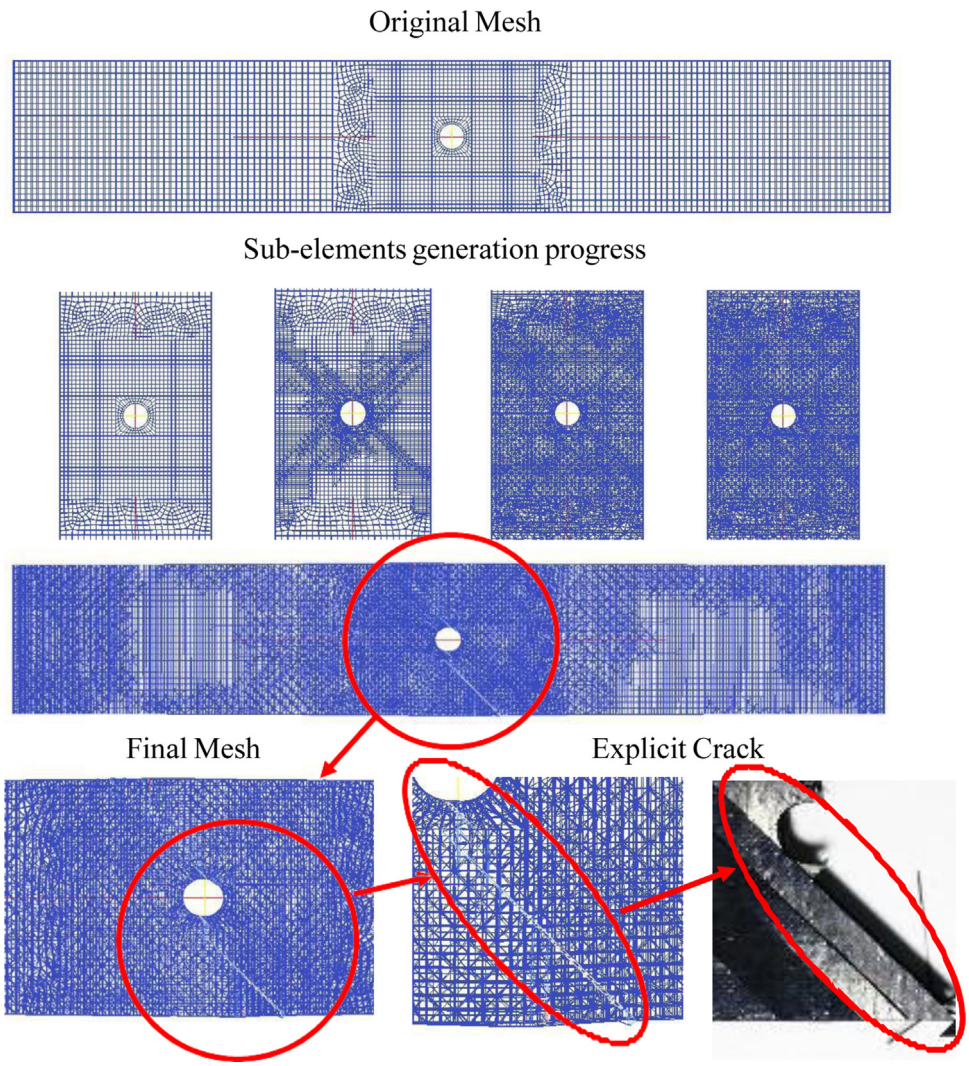

Figure 15 – Sub-elements generation progress of specimens [$45_3/90_3/-45_3/0_3$].

(4) The boundary condition is set to 15 mm/s, the maximum increment step of 0.0025, and there are 4813 elements of the notched single layer. All elements must be hexahedral elements.

4.2. Simulation results of notched laminates [$45_3/90_3/-45_3/0_3$]s

It can be found from the stress strain curve Fig. 14 that the stress curve is not smooth but zigzag in the change of the increasing strain, which is very consistent with the test phenomenon. It can be seen from the Fig. 15, Figure 16and Fig. 17, the simulation results is also mainly delamination and fiber fracture modes. Around the hole, a lot of new elements were generated, and most of them were along 45°, which can be thought as crack propagation.

As a comparison, the red curve in Fig. 14 shows (using the same constitutive law) the failure strength with In-Situ effect is higher than the unmodified one, which is more approximate to the experiments results. The prediction by using the theory of In-Situ strength is in good agreement with the test value. The predicted failure modes also include matrix failure, fiber failure and delamination failure.

It shows that in the case of without considering In-Situ theory, the failure initiation's prediction of notched laminates, significantly lower than the test values, and the prediction of failure strength compared with the experimental results are in good agreement, slightly lower than the results of considering In-Situ effects.

This is because the local strength has a great influence on the initial failure of the matrix and a relatively limited influence on the fiber fracture failure mode.

Therefore, considering the In-Situ effect of laminates in the strength analysis method is helpful to improve the accuracy and calculation precision of failure initiation prediction and make the strength analysis method more reliable.

4.3. Simulation results of notched laminates $[45/0/-45/90]_{3s}$

The stress-strain curves in Fig. 19 are more smooth than the curves in Fig. 14. This is because the layers are laid in

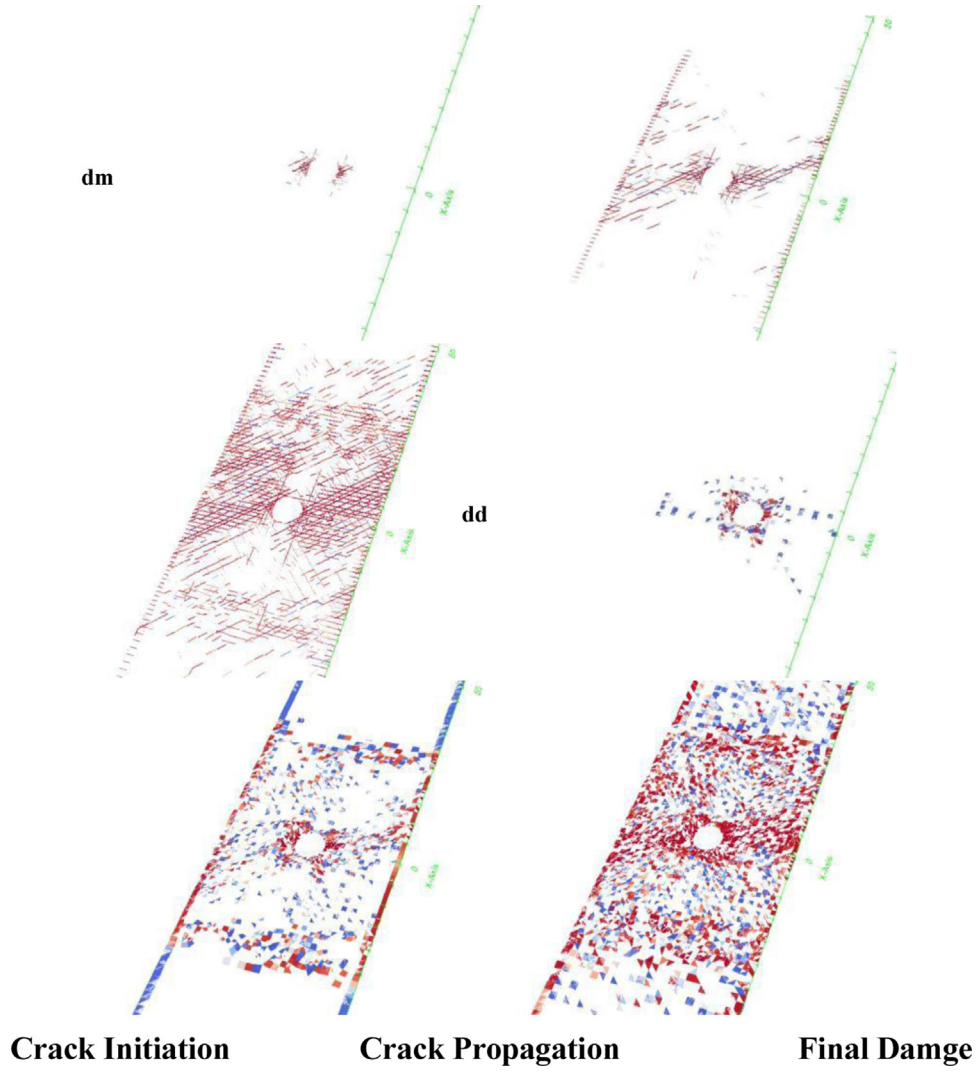

Figure 16 – the damage cloud of delamination and matrix of specimen $[45_3/90_3/-45_3/0_3]_s$.

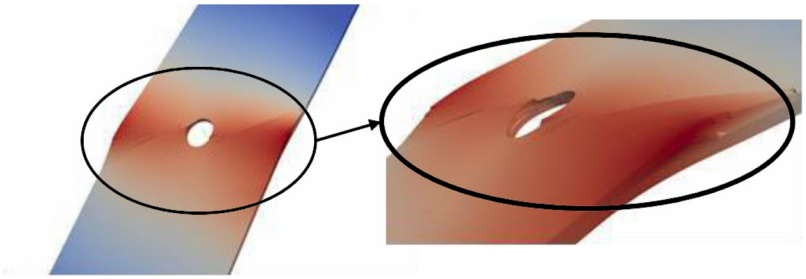

Figure 17 – The stress cloud of FNM results.

alternating order, with low degree of anisotropy and higher uniformity. The delamination is not obvious, and there is only obvious failure mode of fiber fracture.

It can be seen from Fig. 18, the simulation results are mainly fiber fracture and matrix cracking. Another phenomenon is that a large number of new elements are generated horizontally around the hole, which can be thought as vertical cracks.

As a comparison, the blue curve in Fig. 19 shows (using the same constitutive law) the failure strength is higher than the unmodified one. The prediction of In-Situ strength is in good agreement with the test results, and the predicted failure modes are mainly fiber fracture and matrix cracking.

It shows that in the case of without considering In-Situ theory, the failure initiation's prediction of notched laminates, significantly lower than the test values, and the prediction of failure strength compared with the experimental results are in good agreement, slightly lower than the results of

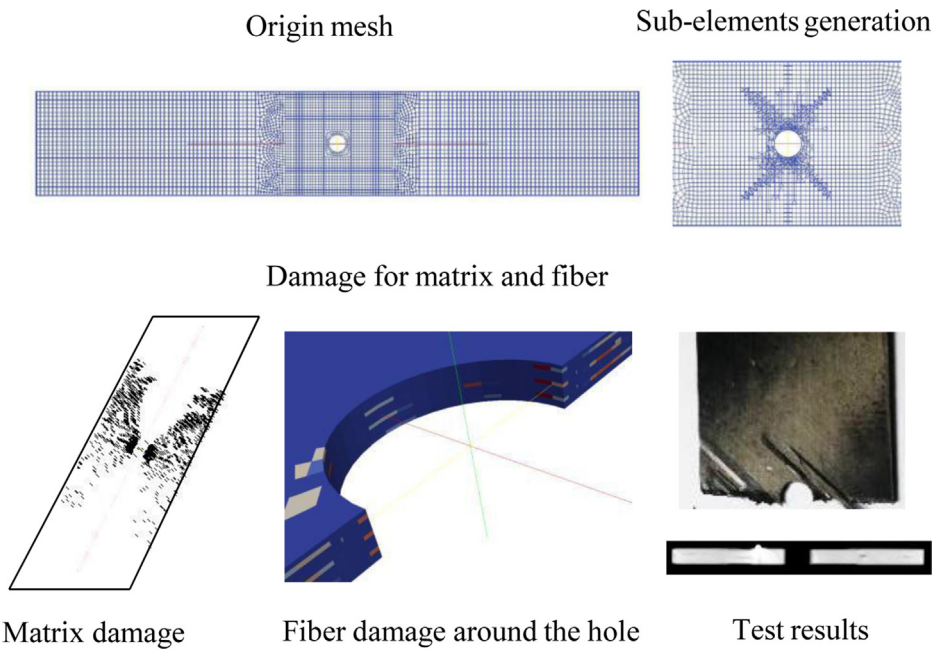

Figure 18 – Sub-elements generation and material damage of specimens $[45_3/90_3/-45_3/0_3]_s$.

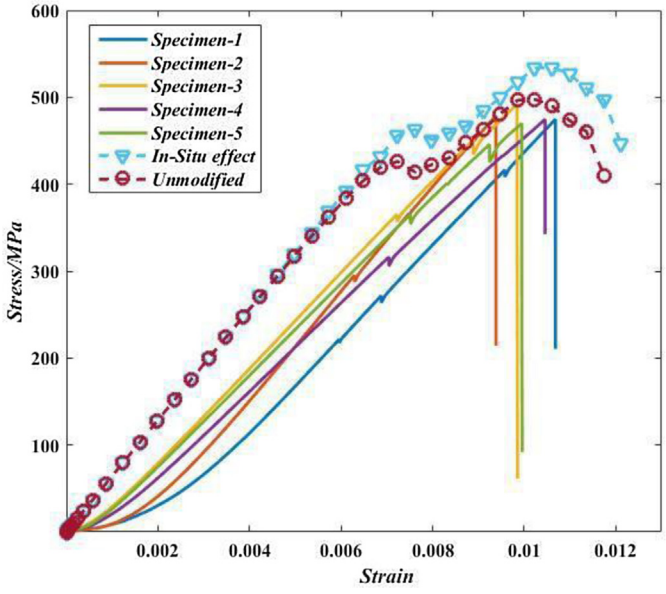

Figure 19 – Simulations and tests' strain-stress curves of specimens $[45_3/90_3/-45_3/0_3]_s$.

considering In-Situ effects, but the overall result is slightly larger than the test result.

5. Conclusions

In this paper, the strength of the test results of specimen $[45_3/90_3/-45_3/0_3]_s$ is slightly lower than specimen $[45_3/90_3/-45_3/0_3]_s$. The main reason is that the middle of the specimen $[45_3/90_3/-45_3/0_3]_s$ is $[0]_6$ as the main load-bearing structure as a thick unidirectional laminates. It can be thought that, although the number of 0° plies are same, if they are consecutive together, the failure strength is higher than the other situations.

The model using floating node method can simulate the crack propagation process explicitly, which is of great help to understand the crack propagation process of composite laminates under tensile load. Two kinds of specimens have different sub-elements generation process. Compared to the experiments results, they are consistent perfectly.

The model using In-Situ theory can significantly improve the accuracy of composite laminates failure strength prediction value. The prediction value of failure strength compared with the experimental results are in good agreement, slightly

higher than the value without considering In-Situ effect. This is mainly because the In-Situ strength does not affect the fiber, but has a great influence on the failure strength of the matrix. Therefore, considering the In-Situ effect of composite laminates is helpful to make the strength analysis method more reliable.

In this paper, the new model using floating node method combined In-Situ effect theory is set up and the final simulation results are in a good agreement with the experiments results. Furthermore, this paper shows the analysis process about the notched composite laminates tensile experiments and simulation method.

6. Conflicts of interest

The authors declare no conflicts of interest.

7. Acknowledgment

This study was supported by the National Natural Science Foundation of China (NO. 11402064), the State Key Program of National Natural Science Foundation of China (NO. 11734017), and the Heilongjiang Postdoctoral Scientific Research Development Fund (NO. LBH = Q17075).

REFERENCES

[1] Reifsnider KL. Some Fundamental Aspects of the Fatigue and Fracture Response of Composite MaterialsC//Proceedings of the Fourteenth Annual Meeting. United States 1977:373–84.
[2] Pinho ST, Iannucci L, Robinson P. Physically-based failure models and criteria for laminated fibre-reinforced composites with emphasis on fibre kinking: part I: development. J Compos Part A - Appl Sci Manuf 2006;37(1):63–73.
[3] Pinho ST, Iannucci L, Robinson P. Physically based failure models and criteria for laminated fibre-reinforced composites with emphasis on fibre kinking. J Part II: FE implementation. Compos Part A -Appl Sci Manuf 2006;37(5):766–77.
[4] Chen BY, Baiz PM, Pinho ST, Tay TE. An extended phantom node method for crack interactions in composites. C In: Proceedings of the 20th UK conference of the association for computational mechanics in engineering. The University of Manchester, Manchester, UK; 2012.
[5] de Borst R. Numerical aspects of cohesive-zone models. J Engng Fract Mech 2003;70(14):1743–57.
[6] Fries T-P, Belytschko T. The extended/generalized finite element method: an overview of the method and its applications. J Numer Meth Engng 2010;84(3):253–304.
[7] Song J-H, Areias PMA, Belytschko T. A method for dynamic crack and shear band propagation with phantom nodes. J Numer Meth Engng 2006;67(6):868–931.
[8] Huynh DBP, Belytschko T. The extended finite element method for fracture in composite materials. J Numer Meth Engng 2009;77(2):214–39.
[9] Chen BY. A floating node method for the modelling of discontinuities in composites. Engineering Fracture Mechanics 2014;127:104–34.
[10] Chen BY. Modelling the tensile failure of composites with the floating node method. Comput. Methods Appl. J Mech. Engrg 2016;308:414–42.
[11] Hettich T, Hund A, Ramm E. Modeling of failure in composites by X-FEM and level sets within a multiscale framework. J Comput Meth Appl Mech Engng 2008;197(5):414–24.
[12] Parvizi A, Garrett K, Bailey J. Constrained cracking in glass fibre-reinforced epoxy cross-ply laminates. J, Journal of Material Science 1978;13(1):195–201.
[13] Dvorak GJ, Laws N. Analysis of progressive matrix cracking in composite laminates II. First ply failure. J, Journal of Composite Materials 1987;21(4):309–29.
[14] Flaggs DL, Kural MH. Experimental determination of the in situ transverse lamina strength in graphite/epoxy laminates. J, Journal of Composite Materials 1982;16(2):103–16.
[15] Sun CT, Tao J. Prediction of failure envelopes and stress/strain behaviour of composite laminates. J. Composites Science and Technology 1988;58(7):1125–36.
[16] Rotem A. Prediction of laminate failure with the Rotem failure criterion. J. Composites Science and Technology 1998;58(7):1083–94.
[17] Chang KY, Llu S, Chang FK. Damage tolerance of laminated composites containing an open hole and subjected to tensile loadings. J, Journal of Composite Materials 1991;25(3):274–301.
[18] Camanho PP, Davila CG, Pinho ST, et al. Prediction of in situ strengths and matrix cracking in composites under transverse tension and in-plane shear. J. Composites: Part A 2006;37(2):165–76.
[19] Song Zhou. Material Orthotropy Effects on Progressive Damage Analysis of Open-hole Composite Laminates under Tension. J. Reinforced Plastics & Composites 2017.
[20] Song Zhou. Progressive Damage Simulation of Open-Hole Composite Laminates under Compression Based on Different Failure Criteria. J. Composite Materials 2017;51(9):1239–51.
[21] Song Zhou. Progressive Damage Simulation of Scaling Effects on Open-Hole Composite Laminates under Compression. J. Reinforced Plastics & Composites 2017.
[22] HB 6740-93 carbon fiber composite laminated laminate open-hole tensile test method. S.